ORIGINAL PRESENTÉ AU WORKSHOP - Février 1998

Correction of the non-linearity of FT remote sensing instruments

Richard L. Lachance†, André Villemaire, and Luc Rochette
BOMEM Inc., 450 St-Jean-Baptiste, Québec, Canada, G2E 5S5

ABSTRACT

Mercury Cadmium Telluride (MCT) photoconductive infrared detector offer state-of-the-art performance in the LWIR spectral range (5 – 16 μm). These detectors are often used in spectroradiometers operating in the LWIR atmospheric window (8 – 12 μm) for remote sensing of distant targets at very low radiance emissions. They offer impressive sensitivity allowing high resolution spectral measurements of wide ranges of targets at moderate temperature. However the non-linearity associated with these detectors is the cause of important radiometric errors in quantitative spectroscopic measurements. The reason for the presence of non-linearity in the detectors has been addressed in a number of publications [1–9]. In Fourier Transform spectroscopy, this non-linear response gives rise to a change of effective responsivity with flux, and also to the presence of undesirable spectral artifacts which cannot be corrected by a simple scaling.

Bomem has developed an advanced method for correcting non-linearities in an MCT detector and associated electronics of a Fourier transform spectroradiometer. The method is a signal processing approach computed in software on measured interferograms. All that is needed is the two standard calibration measurements plus one supplementary measurement of calibrated blackbody in the expected range of temperatures. A set of correction coefficients are then computed from the in-band information by a specialized characterization algorithm, and these coefficients can afterwards be utilized for the correction of any subsequent measurement of the same detector operating under similar conditions. The method has been tested on a Bomem MR200 and the results are discussed below.

Keywords: Non-linearity correction, FTIR, mercury-cadmium-telluride (MCT) detector, spectroscopic accuracy.

1. INTRODUCTION

For an accurate spectrum measurement, it is important to record a signal that is exactly proportional to the corresponding radiation intensity striking the instrument detector. Non-linearities in available infrared detectors and in the electronics of the signal processing circuitry cause distortions in the Fourier transform of a measured interferogram, resulting in a warped spectrum affected by spectral artifacts. As a result, the spectrum generated by infrared FT spectrometers is inaccurate, and corrections must be made in order to respect the allowed error budget.

The mercury-cadmium-telluride (MCT) detector used in Fourier transform spectrometry is a semiconductor element cooled with liquid nitrogen. Its electric resistance changes with the incident IR radiation. Measuring it requires an appropriate circuit and electronic amplification. The strongest non-linearity effect is observed in the center of the interferogram (the area of lowest spectral resolution), creating a disturbing effect on the corresponding baseline. At high radiation density, one cause of non-linear response is the decline in the lifetime of the charge carriers as a result of Auger recombination [7]. If the system bandwidth is adjusted to less than one octave, ghost signal become visible above and below the detector cutoff frequencies; if the detector has a wider band, these spectral artifacts can be surimposed inside the band, disturbing the computed spectrum [5].

1.1 Various correction methods

Non-linearity behavior is observed in photoconductive MCT detectors, whether they are operated using constant current or constant voltage. The voltage applied to the photosensitive area of a constant-voltage biased PC MCT is not constant, because there exists a series resistance internal to the detector that does not change with illumination. This gives rise to an effective change of bias on the photosensitive area with changing illumination, and thus non-linearity. Positive feedback circuits have been proposed to compensate for this effect but have been used with limited success. In fact, even such a circuit causes non-linearity, independent of the intensity of the illumination [7, 8].

† Further author information –
Authors can be reached by phone (418) 877-2944, by fax (418) 877-2834, or by email at the following addresses:
richard.lachance@bomem.com, andre.villemaire@bomem.com, luc.rochette@bomem.com

In parallel to the hardware solution, many signal processing approaches (algorithmic corrections) have been examined in the past, but it appears that most of the methods have been devised for a specific practical problem. The specificity of these methods often makes them applicable only within a restricted domain of application. For example, reference [1] discusses a method applicable when the two outputs of the Michelson interferometer are used to record the interferogram. When only a limited spectral band is measured, reference [3] discusses an iterative convergent method that extract the non-linear phase dependence, references [4] and [6] discuss methods using spectrum above and below the cutoff frequency of the detector and minimization of out-of band spectral artifacts. Patents have been devised on these ideas, among which we can cite [9].

These ideas can be helpful in giving directions for other correction methods, but most of these cannot be used in a general case. We propose in this paper a general purpose algorithm for compensating non-linearities, in the sense that it can work with a wide range of interferogram types (decimated, filtered, etc.), and doesn't need the information outside the detection band, when the spectral artifacts and the global flux (*dc* offset) are not available. The present method is easily computable and does not require large signal processing resources; a characterization step must be first computed for a given detector, requiring three calibration measurements. Afterwards, the computed non-linear correction is valid as long as the sensor optical configuration stays the same or the instrument self radiance does not change.

2. ASCM NON-LINEARITY CORRECTION ALGORITHM

The non-linearity correction method presented in this paper is named the Adaptive Scaling Correction Method (ASCM). It is based on original interferogram measurements. This avoids problems associated with phase correction and information loss during the calibration process. ASCM necessitates at least three measurements of reference blackbodies to quantify the non-linear response of a given detector.

The ASCM consists in correcting the raw interferograms during the processing of the data coming from the instrument, before applying the calibration equations. No assumption is made about the phase, except that the instrument phase must remain the same during the three reference measurements (as it is the case for any calibration method). The non-linear behavior is modeled by a series expansion. The essential feature of the algorithm is an iterative characterization step that extracts the non-linear coefficients describing the non-linear response of a given detector with its associated amplification algorithm, base on a hot, cold, and an intermediate measurement of a blackbody reference. Once the system has been characterized, the computed set of coefficients is applied for the correction of any subsequent measurements.

The method has proved to be independent on the field stop size, and can therefore be applied for any subsequent range of incident flux. This is because the characterization step leads to a transfer function directly relating non-linear to linear flux. The method therefore allows correction for a wide range of blackbody calibration and scene temperatures, that can depart significantly from the ones used during characterization for example.

2.1 General framework

The photon flux of a given scene incoming on a detector can be separated into a *dc* component and a modulated or *ac* component. We can see this as an interferogram $I^{ac}(x)$ added to a signal I^{dc} independent of x the optical path difference. This constant offset includes the photon fluxes coming from the scene and the optical components in the front of the interferometer that are not modulated by the beamsplitter, as well as the stray photon flux coming from surfaces seen after the beam recombiner. Hence $I(x)$ can be written as:

$$I(x) = I^{ac}(x) + I^{dc} \qquad (1)$$

We define here I as the true interferogram, and I_m as the measured one, perturbed by non-linearity. Ordinarily, the *dc* component is removed by the ADC electronics, and only the *ac* portion is available from the measuring instrument, that is I_m^{ac}. This constitutes the detected signal and corresponds to the measured photon flux modulated by the interferometer.

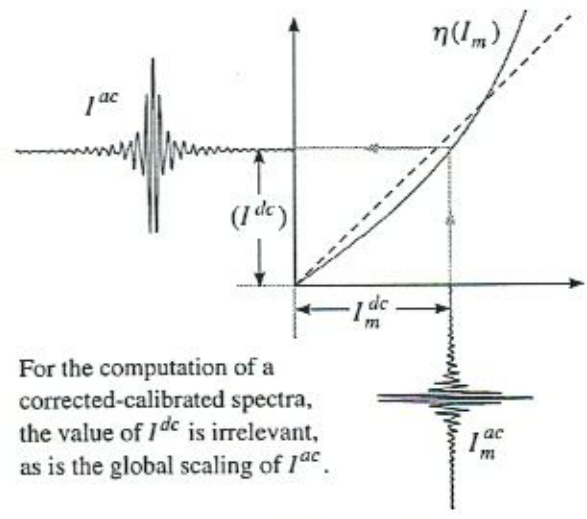

For the computation of a corrected-calibrated spectra, the value of I^{dc} is irrelevant, as is the global scaling of I^{ac}.

Figure 1: Non-linearity transfer function

We base our study on the assumption that the value of I^{dc} is not available. One can then express a generic non-linearity correction operator η, acting on measured interferograms:

$$I(x) = \eta(I_m(x)) \tag{2}$$

The exact form of the operator η is still general at this point. We also assume that this operator does not change for a given detector operating under constant conditions (i.e. constant instrument temperature). The goal of our study is to find the specific expression of η and find a numerical solution that would effectively correct the non-linearity of any interferogram measured by a given characterized detector.

2.2 Calibration equation

The basic approach for determining absolute radiance measured by a FTIR spectrometer is the same as that used for filter radiometers and has been used successfully for other interferometric applications [10]. The detectors and electronics are designed to yield in principle an output which is linear in the incident radiance for all wavenumbers in the optical passband of the instrument, and two reference sources are viewed to determine the slope and offset which define the linear instrument response at each wavenumber.

The measurement obtained by the system is proportional to the spectral power distribution at the detector. The latter is composed of the emission coming from each input port, along with thermal emission of the spectrometer. The measurement can be expressed as:

$$\overline{M} = \overline{G}\,(L + \overline{O}) \tag{3}$$

where $\overline{M}$ is the calculated complex spectrum from the measurement.
L is the true incident spectral radiance from the *scene*.
$\overline{G}$ is the overall responsivity of the instrument, referred to as *gain*.
it is a complex function to include interferogram phase delays,
$\overline{O}$ is the instrument emission, referred to as *offset*,
it is the stray radiance, including all modulated radiance that does not come from the scene.

Overbars refers here to complex quantities, comprising a real and an imaginary part.

Equation (3) expresses the linear relationship between the true spectral radiance L and the measured, uncalibrated spectrum $\overline{M}$. Two non-equivalent calibration observations made at temperature T_C and T_H (subscripts C and H refer to the cold and hot measurements) are required in order to determine the two unknowns, that are the gain $\overline{G}$ and the offset radiance $\overline{O}$ as defined in Equation (3). The offset is the radiance which, if introduced at the input of the instrument, would give the same contribution as the actual emission from various parts of the optical train.

Equation (3) written for both the hot and cold blackbody can be solved to yield:

$$\overline{G} = \frac{\overline{M}_H - \overline{M}_C}{L(T_H) - L(T_C)} \quad \text{and} \quad \overline{O} = \frac{\overline{M}_C\, L(T_H) - \overline{M}_H\, L(T_C)}{\overline{M}_H - \overline{M}_C} \tag{4}$$

where $L(T)$ is the calculated blackbody radiance, modeled to be equal to Planck's equation, multiplied by the emissivity of the blackbody. By inverting Equation (3), one can derive the calibration equation used to convert a spectrum from an unknown scene into calibrated data:

$$L = \frac{\overline{M}}{\overline{G}} - \overline{O} \tag{5}$$

If no error distorts the measurement, this expression for the calibrated radiance leads to a L with no imaginary part.

2.3 Non-linearity characterization

Equations (3), (4), and (5) apply to ideal, linear instruments. If non-linearity is present, like it is often the case for MCT photoconductive detectors, more calibration measurements are requires to solve the radiometric equation. In this case, the calibration Equation (3) can be rewritten with the help of Equation (2) as:

$$\mathcal{F}\{\eta(I_m)\} = \overline{G}(L + \overline{O}) \tag{6}$$

$\mathcal{F}\{\}$ is the Fourier transform operator, converting interferograms into equivalent spectra.

the function η can be expressed with only one coefficient, in other words one additional unknown, then three ent measurements are sufficient to solve Equation (6). In practice, no more than three measurements are necessary se the interferograms contain many points, allowing to find a solution even when the operator η contains more than nknown. Solving for the gain, we obtain:

$$\frac{\mathcal{F}\{\eta(I_M)-\eta(I_C)\}}{L(T_M)-L(T_C)} = \frac{\mathcal{F}\{\eta(I_H)-\eta(I_C)\}}{L(T_H)-L(T_C)} \tag{7}$$

he subscript M refers to the third measurement made at a temperature $T_C \neq T_M \neq T_H$. Equation (7) can be written into uivalent form in which we can neglect the blackbody emissivities (because they cancel one another). The idea is o solve this equation for η. In order to do this we use a minimization algorithm applied on the residual form of the fied Equation (7):

$$\text{Minimize}\left\{\sum_{\sigma=\sigma_{\min}}^{\sigma_{\max}}\left[\left|\frac{\mathcal{F}\{\eta(I_M)-\eta(I_C)\}}{\mathcal{F}\{\eta(I_H)-\eta(I_C)\}}\right|-\left(\frac{L(T_M)-L(T_C)}{L(T_H)-L(T_C)}\right)\right]^2\right\} \tag{8}$$

simplex algorithm [11] is used to minimize Equation (8) and compute the coefficients associated with η. The sums uared residuals are computed between specific spectral limits, defined as $\sigma_{\min}$ and $\sigma_{\max}$. These values can be set to the cal spectral limits of the detector, or restricted to a shorter range to increase precision for specific measurements. This the correction can be tailored to be more effective over a given spectral range. Within the defined range, exclusion ns can also be specified. Such special sub-windows are used to exclude regions where measurement is affected by noise levels or where measurement contains uncertain data, like the 2280 – 2400 cm^{-1} CO_2 window, or the 1250 – cm^{-1} water window for example.

our study, we have used a polynomial expansion for the non-linear correction operator η, developed around I_m^{dc}. forms of this operator can also be used; the ASCM is not restricted to this particular form. As a constant term does ffect the processing of an interferogram, and as the term associated with the first power is canceled in the calibration the chosen form of the polynomial expansion can be expressed as:

$$\begin{aligned}\eta(I_m) &= I_m + \sum_{i=0}^{N-2} d_i\,(I_m)^{i+2} \\ &= (I_m^{dc}+I_m^{ac}) + d_0\,(I_m^{dc}+I_m^{ac})^2 + d_1\,(I_m^{dc}+I_m^{ac})^3 + \ldots\end{aligned} \tag{9}$$

also $\eta(I_m) = \dfrac{I_m}{1 + d_0 I^{dc} + d_1 I^{dc^2} + \ldots}$

e N is the order of the polynomial expansion (in our case, it has been fixed to $N = 4$, leading to the three non-linear ction coefficients d_0, d_1, and d_2). In the case of an ideal system, the coefficients d_i take finite values and remain ant in time.

/e note that the η operator depends on the constant offset of a given interferogram. This means that the amount of ction will vary from one interferogram to another. As the constant offset of a measured interferogram is typically not vn, we derive an estimator of this value by a integration of its coarse spectrum over the full available spectral range. lo this by computing the Fourier transform of a limited number of points around the ZPD region (taken as 256 for tudy):

$$I^{dc} \equiv \int_{\sigma=0}^{8000\ cm^{-1}} \mathcal{F}_{NZPD}\left\{I^{ac}(x)\right\} d\sigma \tag{10}$$

his evaluation of the constant offset is not perfect, and can be affected by numerous sources of errors. Nevertheless, a tant error on the evaluation of I^{dc} has only a small impact on the performance of the ASCM algorithm. According to esults, this definition is sufficient for a good correction, as the ASCM method can successfully converge to a set of uate correction coefficients under various dissimilar conditions.

f numerical filtering of the interferogram is used, scrambling occurs the interferogram points and some information be lost. For example, when gaps exist between the numerical and instrument pass-band filters, this leads to signal in the transmitted interferogram. We have shown that for such a case it was possible to simply use the difference een the maximum and the minimum points of the interferogram as an satisfactory *dc* indicator for the ASCM ction method [5].

2.4 Non-linearity correction

he computation of the d_i coefficients in the characterization phase (solution of Equation (8)), every subsequent red interferogram can be corrected with the η operator (Equation (9)), and be inserted in the calibration (Equation eading to corrected calibrated spectra within the initial specified spectral range (σ_{min} and σ_{max}) used in the terization phase. It is important to note that the η operator leads to corrected interferogram valid only for the use in libration equation. This means that the corrected uncalibrated interferograms and corresponding spectra may have ngless scalings, or irrelevant outside bands structures, caused by secondary artifacts introduced by the method; the l only optimizes data within the range σ_{min} and σ_{max}.

3. EXPERIMENTAL RESULTS

terferograms presented in this paper were measured with a Bomem MR200 interferometer equipped with a MCT InSb detector. Each interferogram result from the coaddition of 100 scans taken at a resolution of 4 cm^{-1}. The le field stop of this instrument was opened to the maximum value possible without saturating detectors, in such a yield to the largest amount of incoming flux and therefore the largest non-linearities. Automatic gains were used, g to optimal amplification factors for the MR200 system.

3.1 InSb measurements

2 presents the raw spectrum magnitude of a measurement of a blackbody at 500°C, as seen by a InSb detector d in arbitrary units). Figure 3 presents the corresponding calibrated spectra in radiance units ([r.u.] = W /(cm^2 sr , using the classical two-point calibration with cold and hot calibration references taken respectively at 400°C and . Measurements were taken with high temperatures blackbodies with a maximum flux level at the limit of saturation InSb detector.

e main curve in Figure 3 represents the radiance amplitude of the calibrated spectrum; in this figure, this spectrum y coincides with the dashed line showing the theoretical blackbody distribution at the measurement's temperature. urve close to zero is the residual imaginary part resulting after calibration. The two vertical lines identify a CO_2 w within the spectral range, this absorption band is more apparent in Figure 2. No importance should be given to sults inside these bands, because of the variability of the CO_2 between measurements. Figure 3 shows that the ation process has been computed with success, as the calibrated curve closely matches the theoretical curve, and as aginary residual remains close to zero. The mean error identified as $<E>$ is defined as the mean of relative errors uted on each point of the spectrum within the specified spectral range. Figure 3 shows that only 0.42% error is t after calibration. The root-mean-square radiometric error is also computed over the same spectral range and is given $_{RMS}$. These indicators all indicate that the level of non-linearity for this type of detector is negligible, as it is expected InSb detector. The transfer function for such a case has been computed and has shown to be practically a straight t 45 degrees. This is not the case for with the MCT detector, as it will be shown in the following section.

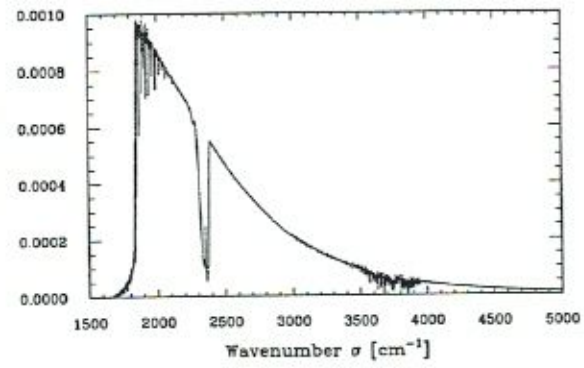

gure 2: Raw InSb detector measurement
T_M = 500°C, 100 coadds, res. = 4 cm^{-1}
F.S. = 1.1 mm, N = 8192

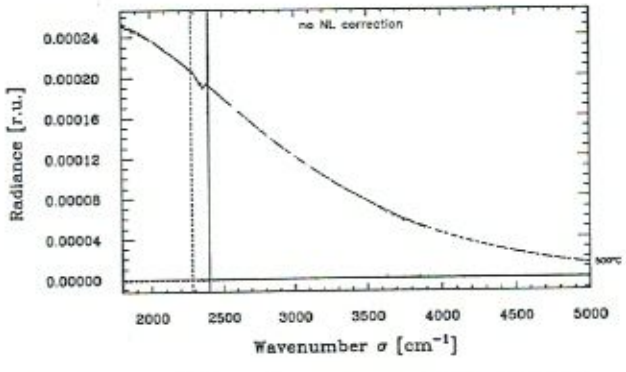

Figure 3: Calibrated measurement, InSb detector
T_C = 400°C; T_M = 500°C; T_H = 600°C
F.S.=1.1 mm, $<E>$=0.42%, E_{RMS}=1.96×10^{-10}

3.2 Short-range MCT measurements

Figure 4 presents the raw spectrum magnitude of a blackbody measurement at 600°C, as seen by a cold-filtered MCT detector. The filter response limits of this detector roughly extend from 700 to 1300 cm^{-1}. From this figure one can see the non-linear quadratic artifacts corresponding in the first order approximation to the autocorrelation of the signal with itself [5]. Signal can be seen at harmonic multiples of the center of the band: one at the origin and one at twice the central frequency of the band (~ 2000 cm^{-1}).

Figure 5 shows the calibrated spectrum when no non-linear correction is performed. As one can see, a large radiometric error is present. This discrepancy leads to a mean relative error of 18%, solely due to the non-linearity of the MCT detector.

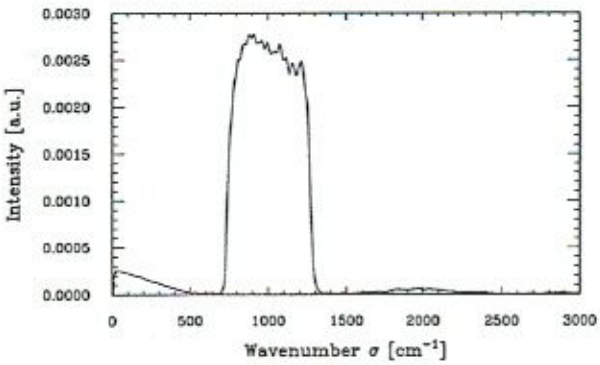

Figure 4: MCT cold-filtered
T_M = 600°C, 100 coadds, res. = 4 cm^{-1}
F.S. = 9.4 mm, N = 8192

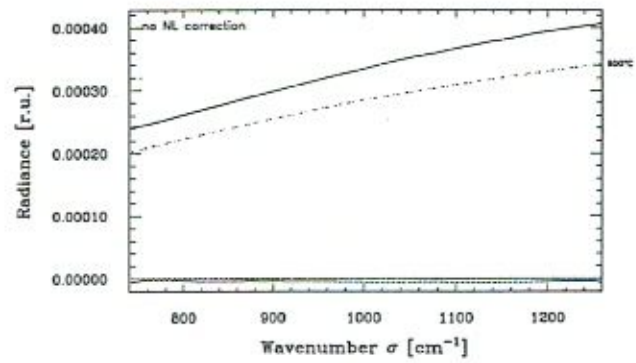

Figure 5: Calibrated measurement (not corrected)
T_C = 300°C; T_M = 600°C; T_H = 900°C
F.S.=9.4 mm, $\langle E \rangle$=18.0%, E_{RMS}=7.1×10^{-7}

The ASCM algorithm is then computed over the range σ_{min} = 740 cm^{-1} to σ_{max} = 1260 cm^{-1}, and a set of correction coefficients are computed from the minimization procedure described in Section 2. Using these coefficients, the calibration is computed again with the ASCM correction and Figure 6 is obtained. The match with the theoretical curve now becomes very good, as indicated by the mean residual error of 0.15%. The normalized transfer function extracted from this characterization is presented in Figure 7. The curvature of the transfer function shows the large amount of non-linearity experienced by this detector.

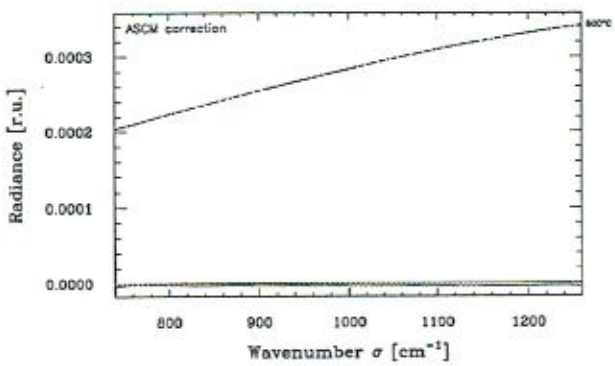

Figure 6: Corrected and calibrated measurement
T_C = 300°C; T_M = 600°C; T_H = 900°C
F.S.=9.4 mm, $\langle E \rangle$=0.15%, E_{RMS}=6.5×10^{-11}

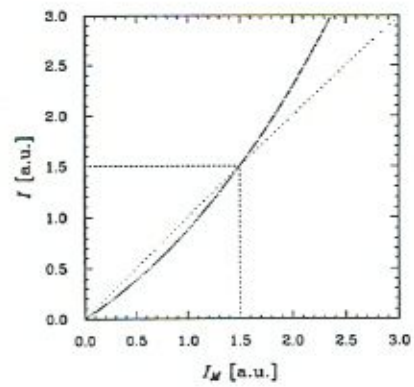

Figure 7: Non-linearity transfer function
MCT cold-filtered
d_0=2.60×10^{-1}, d_1=2.88×10^{-2}, d_2=1.40×10^{-2}

Many test cases were studied with various combinations of blackbody calibration temperatures taken within the range 300°C to 900°C. The characterization computed with the three reference measurements at T_C=300°C, T_M=600°C, T_H=900°C has shown to correctly describe the non-linearity of the cold-filtered MCT detector, applied to any of these other tests and confirmed by a mean residual error always remaining below 1%. Figure 8 demonstrates a typical case of this behavior; using the previous correction coefficients computed for Figure 7, but now using different calibration measurements at T_C=400°C, T_H=800°C and a scene at T=700°C; the ASCM method permits to lower the error from 4.5% down to 0.13%. It is preferable that the calibration temperature range remains limited within the characterization range

(although it can extend a little outside); this is why best results are obtained when the characterization is computed over the largest temperature range possible, in order to cover the widest range of photon flux values.

Figure 9 was computed with still the same original characterization coefficients, but now with a smaller field stop opening of 4.5 mm, with a measurement T=500°C, and calibration points at T_C=300°C and T_H=700°C. In this case of lower flux level, the ASCM correction method leads to a lowering of the radiometric error from 9.7% down to 0.45%. This shows that the ASCM characterization is transferable under different conditions.

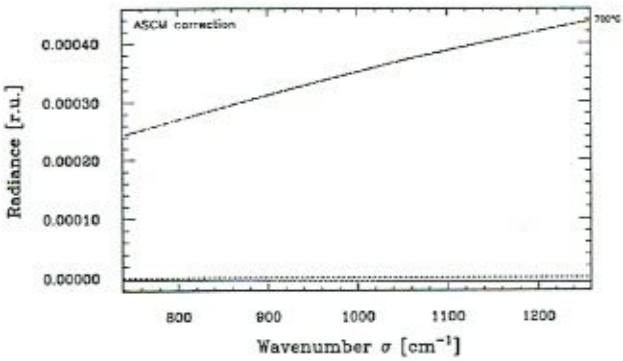

Figure 8: Corrected and calibrated measurement
T_C = 400°C; T = 700°C; T_H = 800°C
F.S.=9.4 mm, <E>=0.13%, E_{RMS}=6.4×10^{-11}

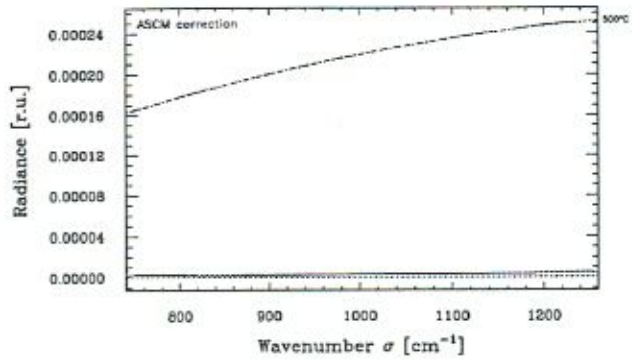

Figure 9: Corrected and calibrated measurement
T_C = 300°C; T = 500°C; T_H = 700°C
F.S.=4.5 mm, <E>=0.45%, E_{RMS}=3.1×10^{-10}

3.3 Wide-range MCT measurements

The ASCM has shown to give quite good non-linear corrections with the use of a band-limited cold-filtered MCT detector, where spectral artifacts are situated outside the detection band. Other tests were made with a wide-band MCT detector, which limits roughly extend from 500 cm^{-1} to over 5000 cm^{-1}. The correction for such a detector is more difficult, especially because of the spectral artifacts superimposed over the whole spectral range.

Figure 10 presents the raw spectrum (uncalibrated) measured with the wideband MCT detector. Some signal can be seen below the detector cutoff, corresponding to out-of-band non-linear spectral artifacts. While the non-linear radiometric deformation is not apparent on such a spectrum, it is much more evident on the calibrated spectrum presented in Figure 11. As one can see from this figure, a large radiometric error is present, causing a mean radiometric error of 24% compute over the displayed spectral range (σ_{min} = 740 cm^{-1} to σ_{max} = 3000 cm^{-1}). The dashed line is the theoretical blackbody distribution at temperature of the measurement. The vertical lines at 1300 cm^{-1} and at 2000 cm^{-1} delimit an H_2O region where absorption lines distort the spectrum.

The ASCM non-linear characterization is then computed with the three-point calibration scheme using references blackbodies at T_C=300°C, T_M=600°C, T_H=900°C, with a field stop opening of 9.4 mm. The transfer function (not shown) obtained is similar to the one presented in Figure 7; the obtained coefficients are d_0=–2.33×10^{-1}, d_1=3.46×10^{-1}, d_2=–7.08×10^{-2}.

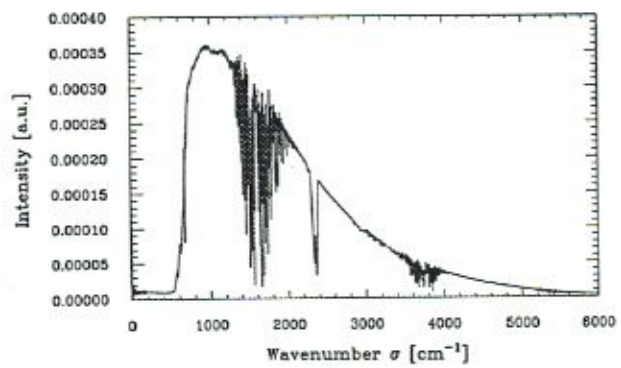

Figure 10: MCT wide-band
T_M = 600°C, 200 coadds, res. = 4 cm^{-1}
F.S. = 9.4 mm, N = 8192

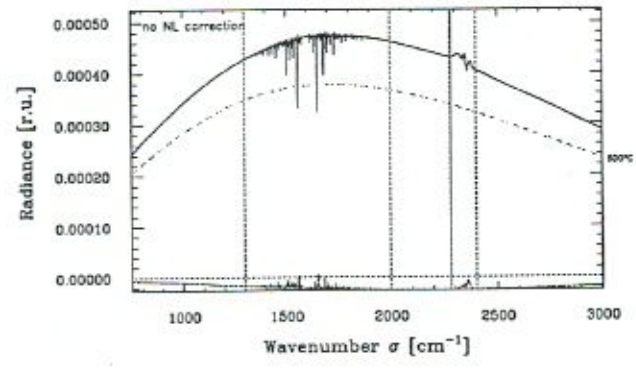

Figure 11: Calibrated measurement (not corrected)
T_C = 300°C; T_M = 600°C; T_H = 900°C
F.S.=9.4 mm, <E>=23.6%, E_{RMS}=3.83×10^{-6}

igure 12 presents the calibrated spectra after non-linearity correction. As one can see, the spectrum distribution now closely matches that of the theoretical blackbody distribution, with a mean relative error smaller than 1 percent over whole given range (except the exclusion windows). The peaks visible in the exclusions windows arise from ction-calibration artifacts due to the H_2O and CO_2 atmospheric absorption bands.

igure 13 presents the calibrated spectra of a blackbody at 800°C measured at a smaller fied stop opening of 4.5 mm, g a cold and hot calibration references at 600°C and 900°C respectively. The ASCM correction is applied with the ious correction coefficients used for Figure 12, and leads to an lowering of the radiometric error from 3.05% down to %. If instead we compute characterization directly at these measurement temperatures and at the photon flux limited ne 4.5 mm field stop opening, the correction yields to an even lower relative error of 0.05%. This shows that the acterization can be tailored to a narrower domain and improve still further measurements taken over a limited range of eratures and photon fluxes.

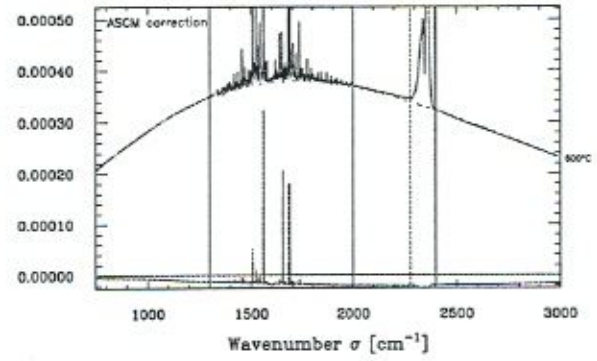

ure 12: Corrected and calibrated measurement
T_C = 300°C; T_M = 600°C; T_H = 900°C
F.S.=9.4 mm, <E>=0.50%, E_{RMS}=2.9×10^{-9}

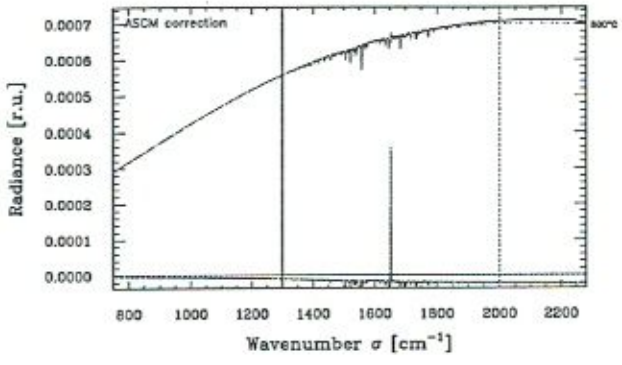

Figure 13: Corrected and calibrated measurement
T_C = 600°C; T = 800°C; T_H = 900°C
F.S.=4.5 mm, <E>=0.57%, E_{RMS}=8.3×10^{-9}

Various tests of transferability of the correction coefficients were made for cases of varying calibration temperatures, stop openings, and spectral optimization range. The transferability has shown to be somewhat less accurate than for ase of the cold-filtered narrow-band MCT detector. However the reduction of the radiometric error by factors between d 50 were observed. The exact improvement obtained depend much on the combination of the cited experimental litions and the chosen spectral range.

3.4 Flame measurements

to now in this paper, the performances of the ASCM algorithm has been demonstrated using only blackbody surements. A natural question that comes to mind is whether the non-linearity correction method can also be used for life measurement, where signal distribution is not smooth, containing high peaks and flat valleys for example. The M corrects the interferogram point by point, as function of the intensity of each bin. Therefore, the shape of the ferogram, and accordingly the shape of the spectrum is of no real importance. In fact, the measured shapes of the raw kbody spectra are not smooth at all, as seen in Figure 4 and especially in Figure 10.

To confirm this assumption, a test was made with a propane flame. The signal was measured with both the InSb and MCT wide-band detectors, and the calibrated signal was compared in the common spectral range extending from 0 cm^{-1} to 4500 cm^{-1}. Figure 14 presents the calibrated spectrum over this range, clearly showing the non-uniform ature. Figure 15 shows a blow-up presenting a superposition of the InSb reference and the corrected MCT surement, corrected with a characterization computed with the three references T_C=300°C, T_M=600°C, T_H=900°C, with eld stop opening of 9.4 mm. As the measured scene has a low flux level, the ASCM correction only achieves a ction of mean relative radiometric error from a factor 2.23% down to 1.01%, compared to the InSb measurement rence. Other tests will have to be done at higher flux levels to confirm more thoroughly the method, but we believe the general scheme of the ASCM method has been demonstrated by these few examples.

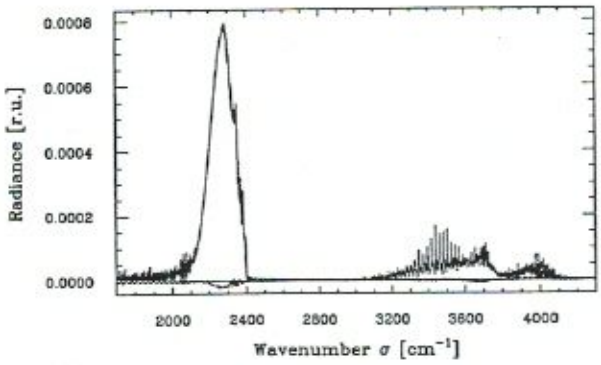

Figure 14: Propane flame measurement, 200 coadds
MCT wide-band, F.S.=9.4 mm
T_C = 300°C; T_C = 400°C

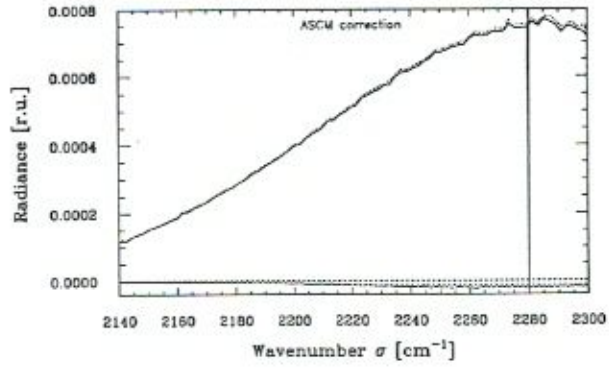

Figure 15: Corrected and calibrated propane measurement
T_C = 300°C; T_H = 400°C
F.S.=9.4 mm, $\langle E \rangle$=1.01%, E_{RMS}=2.30×10^{-8}

4. CONCLUSION

We have derived an algorithmic method for compensating non-linearities in a spectrometer that offer significant accuracy of correction and that requires relatively low resources and time. The generation of the correction coefficients through the η computation during the characterization phase takes between 10 and 30 seconds on a 486-class computer, and this characterization needs to be computed only once. The subsequent correction then takes the same time than the classic calibration computation, and thus it is quite transparent to the user.

In accordance with the ASCM method, a series of correction polynomial coefficients are calculated from reference raw interferograms of three different blackbodies, and these correction factors are then used to calculate a corrected interferogram. Contrary to other non-linear correction methods, the ASCM is not based on outside band spectral artifacts. No restriction is made on the spectral range of the detector (cutoff frequencies) nor on the resolution employed. The algorithm builds constant offset indicator from the measured interferograms, that can be filtered or decimated, as it is often the case for space-borne instruments. This method is versatile; it can be recomputed as often as necessary, for different utilized detectors, used under different studied photon flux ranges (change in detector illumination). The ASCM method can be computed in post-processing, as many times as necessary if the characteristics of the detector change in time for example.

The non-linear correction operator η can be adjusted for different needs, as the analytical form and the number of coefficients for polynomial expansion can be modified. This operator depends on a constant flux indicator I^{dc}, that can be assessed by different methods. We have proposed in this paper a specific form for the η operator and for the evaluation of I^{dc} that have shown to give good results. A very small set of coefficients (3 have shown to be sufficient) are enough to characterize a non-linear MCT detector, and to provide the necessary means to correct all subsequent measurements within a wide range of operation. Further improvements can still be implemented in order to render the ASCM method more powerful. For example, instead of working with only three reference temperatures during the characterization step, a minimization working with many reference blackbody measurements could be used instead to increase the precision and the range of applicability of the computed correction coefficients.

Experimental results obtained in the case of a cold-filtered MCT detector over the range 740 cm^{-1} to 1260 cm^{-1} have shown that is was possible to bring the relative radiometric error of photoconductive MCT detectors on the same range as the accuracy obtained with InSb detectors. Tests with a wide-band detector have shown similar results, using an appropriate spectral range selection within the detector limits.

REFERENCES

1. G. Guelachvili, "Distortion free interferograms in FT spectrometry with non-linear detectors", Appl. Opt., Vol. 25, No. 24, pp. 4644–4648, Dec. 1986.

2. H. E. Revercomb, "Techniques for avoiding phase and non-linearity errors in radiometric calibration: a review of experience with airborne HIS and ground-based AERI", Proceedings of the 5th Workshop on Atmospheric Science from Space using Fourier Transform Spectrometry (ASSFTS), Tokyo, pp. 353–378, 30 Nov. – 2 Dec. 1994.

3. S. Muller, "Correction of non linearity and phase error in IASI interferograms", Proceedings of the 5th Workshop on ASSFTS, Tokyo, pp. 393–406, 30 Nov. – 2 Dec. 1994.

4. M. C. Abrams, G. C. Toon, and R. A. Schindler, "Practical example of the correction of FT spectra for detector non-linearity", Appl. Opt., Vol. 33, pp. 6307 – 6314, 1994.5. A. Villemaire, "MIPAS detector non-linearity correction", Proceedings of the 7th Workshop on ASSFTS, Oberpfaffenhofen, 12–14 May, 1997.

6. P. Jeseck, C. Camy-Peyret, T. Hawat, and S. Payan, "Detector nonlinearity correction scheme for the LPMA balloon-borne Fourier Transform Spectrometer", Proceedings of the 7th Workshop on ASSFTS, Oberpfaffenhofen, 12–14 May, 1997.

7. K. Rahmelow, "Electronic influences on an infrared detector signal: nonlinearity and amplification", Appl. Opt., Vol. 36, No. 10, pp. 2123 – 2132, April 1997.

8. R. A. Shindler, "Correcting for nonlinearity in a photodetector", NASA Tech Brief Vol. 10, No. 2, Item #52, from JPL Invention Report NPO-16055/5509, March 1986.

9. A. Keens, A. Simon, "Correction of non-linearities in detectors in Fourier Transform Spectroscopy", United States Patent number 4927269, May 22, 1990.

10. H. E. Revercomb, H. Buijs, H. B. Howell, D. D. Laporte, W. L. Smith, and L. A. Sromovsky, "Radiometric calibration of IR Fourier transform spectrometers: solution to a problem with the High-Resolution Interferometer Sounder", Appl. Opt., Vol. 27, No 15, pp. 3210–3218, Aug. 1988.

11. M. S. Caceci and W. P. Cacheris, "Fitting curves to data: The Simplex algorithm is the answer", BYTE Magazine, pp. 340–362, May 1984.